



Published in final edited form as:

*Cell Tissue Res.* 2008 November ; 334(2): 243–254. doi:10.1007/s00441-008-0690-9.

## IGF-I regulates tight-junction protein claudin-1 during differentiation of osteoblast-like MC3T3-E1 cells via a MAP-kinase pathway

**Naoko Hatakeyama, Takashi Kojima, Kousuke Iba, Masaki Murata, Mia M. Thi, David C. Spray, Makoto Osanai, Hideki Chiba, Sumio Ishiai, Toshihiko Yamashita, and Norimasa Sawada**

*N. Hatakeyama, K. Iba, T. Yamashita, Department of Orthopaedic Surgery, Sapporo Medical University School of Medicine, S1, W17, Sapporo 060-8556, Japan*

*N. Hatakeyama, T. Kojima, M. Murata, M. Osanai, H. Chiba, N. Sawada, Department of Pathology, Sapporo Medical University School of Medicine, Sapporo, Japan, e-mail: ktakashi@sapmed.ac.jp*

*M. M. Thi, D. C. Spray, Department of Neuroscience, Albert Einstein College of Medicine, Bronx, N.Y., USA*

*S. Ishiai, Department of Rehabilitation, Sapporo Medical University School of Medicine, Sapporo, Japan*

### Abstract

Insulin-like growth factor I (IGF-I) is expressed in many tissues, including bone, and acts on the proliferation and differentiation of osteoblasts as an autocrine/paracrine regulator. Tight-junction proteins have been detected in osteoblasts, and direct cell-to-cell interactions may modulate osteoblast function with respect, for example, to gap junctions. In order to investigate the regulation of expression of tight-junction molecules and of function during bone differentiation, osteoblast-like MC3T3-E1 cells and osteocyte-like MLO-Y4 cells were treated with IGF-I. In both MC3T3-E1 cells and MLO-Y4 cells, the tight-junction molecules occludin, claudin-1, -2, and -6, and the gap-junction molecule connexin 43 (Cx43) were detected by reverse transcription with polymerase chain reaction. In MC3T3-E1 cells but not MLO-Y4 cells, mRNAs of claudin-1, -2, and -6, Cx43, and type I collagen, and proteins of claudin-1 and Cx43 were increased after treatment with IGF-I. Such treatment significantly decreased paracellular permeability in MC3T3-E1 cells. The expression of claudin-1 in MC3T3-E1 cells after IGF-I treatment was mainly upregulated via a mitogen-activated protein (MAP)-kinase pathway and, in part, modulated by a PI3-kinase pathway, whereas Cx43 expression and the mediated gap-junctional intercellular communication protein did not contribute to the upregulation. Furthermore, in MC3T3-E1 cells during wound healing, upregulation of claudin-1 was observed together with an increase of IGF-I and type I collagen. These findings suggest that the induction of tight-junction protein claudin-1 and paracellular permeability during the differentiation of osteoblast-like MC3T3-E1 cells after treatment with IGF-I is regulated via a MAP-kinase pathway, but not with respect to gap junctions.

### Keywords

IGF-I; Tight junction; Claudin-1; Osteoblast; MAP-kinase; Cell culture (murine)

## Introduction

Direct cell-to-cell interactions through cadherin-based adherens junctions and communicating junctions, viz., gap junctions, may modulate osteoblast function by regulating the abundance or movements of signaling molecules or transcriptional factors (Stains and Civitelli 2005). Furthermore, tight-junctional structures coexist with gap-junctional structures between osteoblasts in early osteogenesis (Soares et al. 1992; Arana-Chavez et al. 1995). The tight junctions in osteoblasts may be important for covering the inactive surface of mineralized bone and separating it from the extracellular space and for the polarized trafficking of bone matrix proteins toward the bone surface. However, the mechanism of regulation of the expression and function of tight junctions in osteoblasts remains unknown.

Tight junctions are the apicalmost components of intercellular junctional complexes in epithelial and endothelial cells. The barrier function of tight junctions regulates the passage of ions, water, and small molecules through paracellular spaces. The fence function of tight junctions prevents intermixing of molecules in the apical membrane with those in the basolateral membrane and maintains cell polarity. Therefore, tight junctions are considered to be essential for the development and maintenance of multicellular organisms (Tsukita et al. 2001; D'Atri and Citi 2002; Balda and Matter 2003; Schneeberger and Lynch 2004). Tight junctions are formed by the integral membrane proteins claudins, occludin, junctional adhesion molecules (JAMs), and tricellulin, and by many peripheral membrane proteins, including the scaffold proteins ZO-1, ZO-2, and ZO-3, plus MAGI-1 and cell polarity molecules ASIP/ PAR-3, PAR-6, and atypical protein kinase C (Tsukita et al. 2001; Tsukita and Furuse 2002; Sawada et al. 2003; Schneeberger and Lynch 2004; Ikenouchi et al. 2005). Occludin was the first reported integral membrane protein of tight junctions and is the most ubiquitously expressed at the apicalmost membranes (Furuse et al. 1993). Occludin-deficient mice display thinning of the compact bone without any abnormalities of serum levels of  $\text{Ca}^{2+}$ ,  $\text{PO}_4^{2-}$ , or parathyroid hormone (Saitou et al. 2000). The claudin family, consisting of 24 members, is solely responsible for forming tight-junction strands and shows tissue- and cell-specific expression of individual members (Tsukita et al. 2001). Recently, claudin-1, -2, and -3 and occludin have been reported to be expressed in osteoblasts (Prêle et al. 2003). Furthermore, rat osteoblasts express mRNAs of claudin-1 to -12, -14 to -20, and -22 and -23 (Wongdee et al. 2008).

Gap-junction channels, composed of proteins termed connexins (Cx), mediate the reciprocal exchange of ions and small molecules of less than 1000 Da, including second messengers such as cyclic AMP,  $\text{IP}_3$ , and  $\text{Ca}^{2+}$  between neighboring cells (Sáez et al. 1986, 1989; Kumar and Gilula 1996; Kojima et al. 2001, 2003). Gap-junctional intercellular communication (GJIC) is thought to play an important role in development, cell growth, and cell differentiation (Loewenstein 1979; Bennett et al. 1991; Berthoud et al. 1992; Yamasaki and Naus 1996; Trosko and Ruch 1998). Cx43, Cx45, and Cx46 are expressed in bone cells (Schiller et al. 1992; Schirmacher et al. 1992; Civitelli et al. 1993; Steinberg et al. 1994). In osteoblastic cells, expression of Cx43 and the mediated GJIC contribute to the expression of osteoblastic differentiation markers, alkaline phosphatase activity, osteocalcin, osteopontin, and core binding factor  $\alpha 1$  (Cbfa1; Li et al. 2006). Gap junctions may be closely associated with tight junctions (Kojima et al. 2003; Giepmans 2004). Some Cx can induce and maintain tight junctions in both a GJIC-dependent and GJIC-independent manner in epithelial cells (Kojima et al. 2007). Cx32 expression and the mediated GJIC can induce the expression of claudin-1 and its function in hepatocytes (Kojima et al. 2002). Cx26 expression can induce expression of claudin-14 and claudin-4 in the cell lines Calu-3 and Caco-2, respectively (Morita et al. 2004; Go et al. 2006). However, interaction between Cx and integral membrane tight-junction proteins in osteoblasts remains unclear.

Insulin-like growth factor-I (IGF-I) is generally known to play an essential role in anabolic regulation of bone metabolism (Canalis 1993; Conover 2000; Olney 2003). Patients with Laron syndrome, caused by IGF-I deficiency, exhibit growth retardation and osteoporosis (Laron et al. 1999). In vitro, IGF-I induces the proliferation and differentiation of osteoblastic cells (McCarthy et al. 1989; Canalis 1993; Farquharson et al. 1993; Zhang et al. 1999). In osteoblast-like MC3T3-E1 cells, IGF-I stimulates the activity of alkaline phosphatase via mitogen-activated protein (MAP)-kinase and PI3-kinase pathways (Noda et al. 2005; Hanai et al. 2006). IGF-I induces the activity of Cbfa1 via a MAP-kinase pathway in MC3T3-E1 (Pei et al. 2003). Furthermore, IGF-I acts as a signal for osteoblast mitogenesis and survival through parallel PI3-kinase and MAP-kinase pathways (Grey et al. 2003).

In the present study, in order to investigate the regulation of the expression of tight-junction molecules and their functions during bone differentiation, osteoblast-like MC3T3-E1 cells and osteocyte-like MLO-Y4 cells were treated with IGF-I. In MC3T3-E1 cells, but not MLO-Y4 cells, IGF-I induced the expression in mRNAs of claudin-1, -2, -6, Cx43, and type I collagen and decreased paracellular permeability. The induction of claudin-1 in MC3T3-E1 cells after treatment with IGF-I was regulated via a MAP-kinase pathway and, in part, modulated by a PI3-kinase pathway.

## Materials and methods

### Cytokine, inhibitors, and antibodies

Murine IGF-I was purchased from PeproTech, (London, UK). A MAP-kinase inhibitor (PD98059), p38 MAP-kinase inhibitor (SB203580), PI3-kinase inhibitors (LY294002 and wortmannin), and protein kinase C inhibitor (GF109203) were purchased from Calbiochem-Novabiochem (San Diego, Calif.). Rabbit polyclonal antibodies to occludin, claudin-1, -2, -6, Cx43, and ZO-1 were obtained from Zymed Laboratories (San Francisco, Calif.). Rabbit polyclonal anti-phospho-MAPK and anti-Akt antibodies and a mouse monoclonal phospho-Akt antibody were purchased from Cell Signaling (Beverly, Mass.). A rabbit polyclonal anti-ERK 1/2 antibody was purchased from Promega (Madison, Wis.). A rabbit polyclonal anti-actin antibody and GJIC blocker 18 $\beta$ -glycyrrhetic acid (18 $\beta$ -GA) were obtained from Sigma (St. Louis, Mo.). Alexa 488 (green)-conjugated anti-rabbit IgG and Alexa 592 (red)-conjugated anti-rabbit IgG were purchased from Molecular Probes (Eugene, Ore.). Horseradish-peroxidase (HRP)-conjugated anti-mouse IgG and HRP-conjugated anti-rabbit IgG were purchased from DAKO (Denmark). The enhanced chemiluminescence (ECL) Western blotting system was obtained from Amersham (Buckinghamshire, UK). <sup>14</sup>C-mannitol and <sup>14</sup>C-inulin were purchased from Amersham Pharmacia Biotech (Piscataway, N.J.).

### Cell culture and treatment

Murine osteoblast-like MC3T3-E1 cells (obtained from Dr. Kenneth J. McLeod, SUNY, Stony Brook) were cultured in  $\alpha$ -MEM medium (GIBCO-BRL, Grand Island, N.Y.) with 5% fetal bovine serum (FBS, Cansera International, Ontario, Canada), 100 U/ml penicillin (GIBCO-BRL), and 100  $\mu$ g/ml streptomycin (GIBCO-BRL). Murine osteocyte-like MLO-Y4 cells (obtained from Dr. Lynda F. Bonewald, University of Texas Health Science Center) were cultured in  $\alpha$ -MEM medium with 10% FBS, 2.5% calf serum (GIBCO-BRL), 100 U/ml penicillin, and 100  $\mu$ g/ml streptomycin. These cells were placed in a 5% CO<sub>2</sub>:95% air incubator at 37°C, grown to confluence, and treated with IGF-I for 24 h after pretreatment with  $\alpha$ -MEM medium containing 0.1% bovine serum albumin (Sigma) without FBS for 18 h. The MC3T3-E1 cells were pretreated with the inhibitors at 30 min before treatment with IGF-I for 24 h.

### RNA isolation and reverse transcription with polymerase chain reaction

Total RNA was extracted and purified by using Trizol (GIBCO-BRL). For reverse transcription with polymerase chain reaction (RT-PCR), 1 µg of total RNA was reverse-transcribed (RT) into cDNA with a mixture of oligo (dT) and SuperScript II reverse-transcriptase under the recommended conditions (Invitrogen, Carlsbad, Calif.). Each cDNA synthesis was performed in a total volume of 20 µl for 50 min at 42°C and was terminated by incubation for 15 min at 70°C. RT-PCR was performed by using 1 µl of the 20-µl total RT product, PCR buffer, dNTPs, and Premix Taq DNA polymerase under the manufacturer's recommended conditions (Takara, Shiga, Japan). Conditions applied for PCR were 96°C for 30 s, 25 or 30 cycles of 96°C for 15 s, 55°C for 30 s, 72°C for 1 min, and 72°C for 7 min on a Perkin Elmer/Cetus Thermocycler Model 2400. Of the 20 µl total PCR, 10 µl was analyzed by electrophoresis in ethidium-bromide-impregnated 1% agarose gel. Primers used to detect type I collagen, osteopontin, osteocalcin, occludin, claudin-1, -2, -3, -4, -5, -6, -7, -8, Cx43, and glucose-3-phosphate dehydrogenase (G3PDH) are indicated in Table 1.

### Western blot analysis

Cultures in 60-mm dishes were washed with phosphate-buffered saline (PBS) twice, and 300 µl buffer (1 mM NaHCO<sub>3</sub>, 2 mM phenylmethylsulfonyl fluoride [PMSF]) was added. The cells were scraped and collected in microcentrifuge tubes and then sonicated for 10 s. The protein concentrations of the samples were determined by using a BCA Protein Assay Reagent Kit (Pierce Chemical, Rockford, Ill., USA). Aliquots of 15 µg protein/lane for each sample were separated by electrophoresis in 4%/20% SDS-polyacrylamide gels (SDS-PAGE; Daiichi Pure Chemicals, Tokyo, Japan). After electrophoretic transfer to nitrocellulose membranes (Bio-Rad Laboratories, Hercules, Calif.), these membrane were saturated for 30 min at room temperature with blocking buffer (25 mM TRIS pH 8.0, 125 mM NaCl, 0.1% Tween 20, 4% skim milk) and incubated with polyclonal anti-claudin-1, polyclonal anti-claudin-2, polyclonal anti-claudin-6, polyclonal anti-Cx43, polyclonal anti-ZO-1, polyclonal anti-phospho-MAPK, polyclonal anti-ERK1/2, monoclonal anti-phospho-Akt, polyclonal anti-Akt, or polyclonal anti-actin antibodies at room temperature for 1 h. The membranes were incubated with HRP-conjugated anti-rabbit or HRP-conjugated anti-mouse IgG (Dako, Tokyo, Japan) at room temperature for 1 h. The immunoreactive bands were detected by using an ECL Western blotting system (Amersham, Buckinghamshire, UK).

### Immunoprecipitation

The dishes were washed with PBS twice, and 300 µl NP-40 lysis buffer (50 mM TRIS-HCl, 2% NP-40, 0.25 mM Na-deoxycholate, 150 mM NaCl, 2 mM EGTA, 0.1 mM Na<sub>3</sub>VO<sub>4</sub>, 10 mM NaF, and 2 mM PMSF) was added to 60-mm dishes. The cells were scraped and collected in microcentrifuge tubes and then sonicated for 10 s. Cell lysates were incubated with protein A-Sepharose CL-4B (Pharmacia LKB Biotechnology, Uppsala, Sweden) for 1 h at 4°C and then clarified by centrifugation at 15,000g for 10 min. The supernatants were incubated with polyclonal anti-claudin-1 or polyclonal anti-Cx43 antibodies bound to protein A-Sepharose CL-4B overnight at 4°C. After incubation, immunoprecipitates were washed extensively with the same lysis buffer and used for Western blot analysis.

### Immunofluorescence microscopy

For immunocytochemistry, cells grown on glass cover-slips, which were coated with rat tail collagen (500 µg dried tendon/ml in 0.1% acetic acid), were fixed with an ethanol and acetone mixture (1:1) or acetone at -20°C for 10 min. After the samples were rinsed with PBS, they were incubated with polyclonal anti-claudin-1 and anti-Cx43 antibodies as primary antibodies at room temperature for 1 h and then with the secondary antibodies, Alexa 488 (green)-conjugated and Alexa 592 (red)-conjugated anti-rabbit IgG, at room temperature for 1 h. The

specimens were examined by using a laser-scanning confocal microscope (MRC 1024; Bio-Rad, Hercules, Calif.). Phase-contrast photomicrographs were taken with a Zeiss Axiovert 200 inverted microscope.

### Freeze-fracture analysis

For freeze-fracture analysis, cells grown on 60-mm dishes were centrifuged into pellets and then immersed in 40% glycerin solution after fixation in 2.5% glutaraldehyde in 0.1 M PBS (pH 7.3). The specimens were mounted on a copper stage, frozen in liquid nitrogen, fractured at  $-150^{\circ}\text{C}$  to  $-160^{\circ}\text{C}$ , and replicated by platinum/carbon from an electron beam gun positioned at a  $45^{\circ}$  angle, followed by carbon applied from overhead in a JFD-7000 freeze-fracture device (JEOL, Tokyo, Japan). After the replicas were thawed, they were floated on filtered 10% sodium hypochlorite solution for 10 min in a Teflon dish. Replicas were washed in distilled water for 30 min, mounted on copper grids, and examined at 80 kV by using a JEOL 1200EX transmission electron microscope (JEOL, Tokyo, Japan).

### Measurement of transepithelial electrical resistance

Cells were cultured to confluence on 12-mm Transwell filters of 0.4  $\mu\text{m}$  pore size (Corning, N.Y.) coated with rat tail collagen. Transepithelial electrical resistance (TER) was measured by using an EVOM voltammeter with an ENDOHM-12 (World Precision Instruments) on a heating plate (Fine, Tokyo, Japan) adjusted to  $37^{\circ}\text{C}$ . Values were expressed in standard units of ohms per square centimeter and presented as the mean  $\pm$  SE. For calculation, the resistance of blank filters was subtracted from that of filters covered with cells.

### Measurement of paracellular flux

Cells were cultured to confluence on 12-mm Transwell filters of 0.4  $\mu\text{m}$  pore size, and  $^{14}\text{C}$ -inulin (MW 5 kDa)-containing or  $^{14}\text{C}$ -mannitol (MW 182 Da)-containing medium was added to the inner chamber after 1 mM unlabeled substrates were added to the medium in the inner and the outer chambers. Samples were collected from the outer chamber at 120 min and were measured with a liquid scintillation counter (Beckman LS-6500). The results were expressed as clearance per h per sequence centimeter (inulin, pmol/h per  $\text{cm}^2$ ; mannitol, nmol/h per  $\text{cm}^2$ ).

### Wound-healing model

MC3T3-E1 cells were grown on 60-mm dishes to confluence and were scratched with a plastic pipette tip. At 6 h, 24 h, and 48 h after scrape wounding, the cells were used for immunocytochemistry and RT-PCR.

### Data analysis

Signals were quantified by using Scion Image Beta 4.02 Win (Scion, Frederick, Mich., USA). Each set of results shown is representative of three separate experiments. Results are given as means  $\pm$  SE. Differences between groups were tested by the two-tailed Student's *t*-test for unpaired data.

## Results

### Expression of tight-junction molecules and Cx43 in MC3T3-E1 and MLO-Y4 cells

To examine the difference in the expression of tight-junction molecules and Cx43 between osteoblasts and osteocytes, RT-PCR analysis for bone differentiation markers, viz., type I collagen, osteopontin, and osteocalcin, and for integral tight-junction molecules, viz., occludin, claudin-1, -2, -3, -4, -5, -6, -7, and -8, and for Cx43, was performed on osteoblast-like MC3T3-E1 cells and osteocyte-like MLO-Y4 cells. In MC3T3-E1 cells, high expression of type I

collagen and osteopontin and low expression of osteocalcin were observed, whereas in MLO-Y4 cells, low expression of type I collagen and high expression of osteopontin and osteocalcin were observed (Fig. 1a). Furthermore, mRNAs of claudin-1, -2, -6, and Cx43 were detected in both MC3T3-E1 cells and MLO-Y4 cells (Fig. 1b). Expression of claudin-1, -2, and -6 was higher in MC3T3-E1 cells than in MLO-Y4 cells (Fig. 1b). Although occludin mRNA was also detected in both cell lines, the expression was very low level (Fig. 1b).

### **Upregulation of claudins, Cx43, and ZO-1 in MC3T3-E1 cells, but not in MLO-Y4 cells, after IGF-I treatment**

To examine the changes in expression of claudins, Cx43, and ZO-1 during bone differentiation, MC3T3-E1 cells and MLO-Y4 cells were treated with 0.1, 1, and 10 nM IGF-I. In RT-PCR, the upregulation of type I collagen, claudin-1, -2, -6, and Cx43 mRNAs was observed after 0.1 nM IGF-I treatment in MC3T3-E1 cells but not in MLO-Y4 cells (Fig. 2a). The expression was highest after 1 nM IGF-I treatment. In Western blotting, the upregulation of claudin-1 and Cx43 proteins, but not claudin-2 and -6 proteins, was observed following 1 nM IGF-I treatment in MC3T3-E1 cells (Fig. 2b). By immunocytochemistry, claudin-1-immunoreactive lines were observed at cell borders of MC3T3-E1 cells treated with 1 nM IGF-I, whereas they were not detected in the control (Fig. 2c-e). Claudin-2 and -6 were not detected in the control or after treatment with 1 nM IGF-I (data not shown). Cx43-positive spots were increased in MC3T3-E1 cells treated with 1 nM IGF-I compared with the control (Fig. 2f,g). Furthermore, ZO-1, which localized at adherens and tight junctions, was also increased following 1 nM IGF-I treatment as shown in Western blotting, and ZO-1-immunoreactive lines at cell borders were increased in MC3T3-E1 cells treated with 1 nM IGF-I compared with the control as shown by immunocytochemistry (supplemental data). In freeze-fracture analysis, several short tight-junction-like strands, which were occupied by chains of particles and many typical gap-junction plaques, were observed at the membrane of MC3T3-E1 cells treated with 1 nM IGF-I (Fig. 2h,i).

### **Inhibition of paracellular permeability in MC3T3-E1 cells after IGF-I treatment**

To elucidate whether claudin-1 induced by IGF-I treatment affected tight-junction function in MC3T3-E1 cells, we performed a barrier function assay measuring TER, and a paracellular permeability assay measuring paracellular fluxes. The values of TER in MC3T3-E1 cells treated with 1 nM IGF-I were only slightly increased compared with the control (Fig. 3a). The paracellular fluxes measured by using <sup>14</sup>C-inulin and <sup>14</sup>C-mannitol were significantly decreased in MC3T3-E1 cells treated with 1 nM IGF-I compared with the control (Fig. 3b,c).

### **Induction of claudin-1 in MC3T3-E1 cells after IGF-I treatment not influenced by either Cx43 expression or GJIC**

To examine whether Cx43-mediated intercellular communication affected the induction of claudin-1 after IGF-I treatment, MC3T3-E1 cells were pretreated with the GJIC blocker 18 $\beta$ -GA before treatment with 1 nM IGF-I. The 18 $\beta$ -GA treatment did not inhibit the upregulation of claudin-1 and Cx43 proteins in cells treated with IGF-I, as shown in Western blots (Fig. 4a). To examine the interaction between claudin-1 and Cx43 induced by IGF-I, co-immunoprecipitation with Cx43 and claudin-1 antibodies was performed. Claudin-1 and Cx43 were not detected in the immunoprecipitates by using Cx43 and claudin-1 antibodies, respectively (Fig. 4b). These results suggest that claudin-1 may be induced by IGF-I in a gap-junction-independent manner.

### Regulation of claudin-1 expression via MAP-kinase and PI3-kinase pathways in MC3T3-E1 cells after IGF-I treatment

To examine which signaling pathways regulated the expression of claudin-1 in MC3T3-E1 cells after IGF-I treatment, MC3T3-E1 cells were pretreated with PD98059 (a MAP-kinase inhibitor), SB203580 (a p38 MAP-kinase inhibitor), LY294002 (a PI3-kinase inhibitor), or GF109203 (a protein kinase C inhibitor) at 10  $\mu$ M before treatment with 1 nM IGF-I. In Western blots, the expression level of pMAP-kinase (44 kDa) but not pAkt was increased together with an increase of claudin-1 expression in MC3T3-E1 cells after IGF-I treatment (Fig. 5a). The increase of pMAP-kinase and claudin-1 expression was inhibited by PD98059, SB203580, or GF109203 (Fig. 5a). Furthermore, the expression level of pMAP-kinase and claudin-1 after IGF-I treatment was enhanced by LY294002, whereas pAkt expression was decreased (Fig. 5a). When MC3T3-E1 cells were pretreated with 0.1–10  $\mu$ M LY294002 before treatment with 1 nM IGF-I, the expression levels of pMAP-kinase and claudin-1 were increased from 0.1  $\mu$ M, whereas pAkt expression was decreased at 10  $\mu$ M (Fig. 5b). Furthermore, when MC3T3-E1 cells were pretreated with another PI3-kinase inhibitor, wortmannin, at 10 nM before treatment with 1 nM IGF-I, an upregulation of pMAP-kinase and claudin-1 expression and a downregulation of pAkt expression were observed (Fig. 5c).

### Induction of claudin-1 expression in MC3T3-E1 cells during wound healing

To examine the change in claudin-1 expression in MC3T3-E1 cells during regeneration, we performed a wound-healing assay in vitro. In wound-closure areas at 48 h after scrape wounding, claudin-1 was localized at cell borders of attached points (Fig. 6b-e). Furthermore, from 24 h after scrape wounding, mRNAs of IGF-I, type I collagen, and claudin-1 were upregulated compared with the control as shown in RT-PCR analyses (Fig. 6f, data not shown).

## Discussion

Tight-junction structures coexist with gap-junction structures between osteoblasts in early osteogenesis (Soares et al. 1992; Arana-Chavez et al. 1995). Tight-junction molecules claudins, occludin, and ZO-1 are expressed in osteoblasts (Laing et al. 2001; Prêle et al. 2003; Thi et al. 2003). In osteoblasts, gap-junction protein Cx43 and mediated GJIC are well known to contribute to the expression of osteoblastic differentiation markers, alkaline phosphatase activity, osteocalcin, osteopontin, and Cbfa1 (Li et al. 2006). However, the changes and mechanism of regulation of tight junctions during the differentiation of osteoblasts remain unknown. In this study, we have demonstrated, for the first time, that the expression of tight-junction protein claudin-1 and paracellular permeability are regulated via a MAP-kinase pathway, but not by Cx43 expression, during osteoblast differentiation stimulated by IGF-I.

Osteocytes are derived from osteoblasts and are formed by the incorporation of osteoblasts into the bone matrix (Franz-Odenaal et al. 2006). There are no classical apical and basolateral domains in the plasma membrane of osteocytes in vitro (Gu et al. 2006). In contrast, in osteoblasts, cell polarity is important for underlying the polarized trafficking of bone matrix proteins toward the bone surface (Prêle et al. 2003). In this study, we have investigated the expression of tight-junction molecules in MC3T3-E1 cells highly expressing type I collagen and in MLO-Y4 cells highly expressing osteocalcin. In both cell lines, mRNAs for tight-junction molecules occludin and claudin-1, -2, and -6 were detected by semiquantitative RT-PCR. Expression of claudin-1, -2, and -6 mRNAs was higher in MC3T3-E1 cells than in MLO-Y4 cells. These results suggest that tight junctions may be essential for osteoblasts, rather than for osteocytes.

The tight-junction molecules claudin-1, -2, -3, and occludin are reported to be more highly expressed in rat primary osteoblastic cells than in rat osteosarcoma cell line ROS 17/2.8 (Prêle

et al. 2003). The expression of claudin-1 and -2 is increased in the mineralization phase compared with the differentiation phase in primary culture (Prêle et al. 2003). Furthermore, a previous study has shown that a lanthanum tracer penetrates the intercellular spaces of osteoblasts in the early nonmineralised stage, and that the penetration then gradually decreases with the progression of mineralization, and eventually fails to reach the distal portion (apical in relation to the matrix) of the intercellular spaces, as shown by electron microscopy (Soares et al. 1992). In the present study, treatment with IGF-I induced claudin-1 expression at the levels of mRNA and protein together with increases of Cx43 and type I collagen in MC3T3-E1 cells but not MLO-Y4 cells. Immunocytochemistry revealed claudin-1 at the cell borders of MC3T3-E1 cells treated with IGF-I. Furthermore, treatment with IGF-I decreased paracellular permeability measured as paracellular fluxes by inulin and mannitol in MC3T3-E1 cells. These results indicate that, during differentiation of osteoblasts, IGF-I might regulate the paracellular pathway between osteoblasts via the tight-junction protein claudin-1.

On the other hand, the increase of TER is only slight in MC3T3-E1 after IGF-I treatment. Overexpression of claudin-1 increases TER and decreases paracellular permeability in MDCK cells, whereas the introduction of claudin-2 into MDCK I cells decreases TER and does not affect the paracellular flux of fluorescein-isothiocyanate-dextran (Inai et al. 1999; Furuse et al. 2001). In our experiments, IGF-I treatment induces not only claudin-1 expression, but also claudin-2 expression in MC3T3-E1 cells. This suggests that the induction of claudin-2 by IGF-I treatment might also affect the TER value in MC3T3-E1 cells.

Gap junctions may be closely associated with tight junctions (Kojima et al. 2003; Giepmans 2004). Some Cx can induce and maintain tight junctions in both a GJIC-dependent and GJIC-independent manner in epithelial cells (Kojima et al. 2002, 2007; Morita et al. 2004; Go et al. 2006). In this study, treatment with the GJIC blocker 18 $\beta$ -GA did not inhibit the upregulation of claudin-1, and interaction between Cx43 and claudin-1 was not observed by co-immunoprecipitation. These results suggest that Cx43 expression and mediated GJIC do not contribute to the upregulation of claudin-1 by IGF-I in MC3T3-E1 cells.

IGF-I induces at least two signaling pathways, the MAP-kinase and PI3-kinase pathways (LeRoith 2000; Laviola et al. 2007). In MC3T3-E1 cells, IGF-I stimulates the activity of alkaline phosphatase via the MAP-kinase and PI3-kinase pathways (Noda et al. 2005; Hanai et al. 2006) and the activity of Cbfa1 via a MAP-kinase pathway (Pei et al. 2003). Furthermore, IGF-I signals osteoblast mitogenesis and survival through parallel PI3-kinase and MAP-kinase pathways (Grey et al. 2003). In our present study, the expression level of pMAP-kinase, but not of pAkt, was increased together with an increase in claudin-1 expression in MC3T3-E1 cells treated with IGF-I. The increase of pMAP-kinase and claudin-1 expression after treatment with IGF-I was inhibited by PD98059, SB203580, or GF109203. The increase of pMAP-kinase and claudin-1 expression was enhanced by the PI3-kinase inhibitors LY294002 and wortmannin. Cross-talk occurs between PI3-kinase and MAP-kinase (Zimmermann and Moelling 1999; Rommel et al. 1999; Reusch et al. 2001; Moelling et al. 2002). In primary porcine tendon fibroblasts pretreated with LY294002 followed by stimulation with IGF-I, pMAP-kinase is enhanced (Chiu et al. 2005). On the other hand, the two PI3-kinase inhibitors, LY294002 and wortmannin, which have different mechanisms of action and different pharmacological profiles, suppress the activity of pMAP-kinase through an independent PI3-kinase pathway (Chiu et al. 2005). In our study, the upregulation of pMAPK and claudin-1 was observed following low doses of LY294002 that did not affect pAkt. Thus, LY294002 might affect the activity of pMAP-kinase through an independent PI3-kinase pathway. These findings indicate that the expression of claudin-1 in MC3T3-E1 cells after treatment with IGF-I is mainly regulated via a MAP-kinase pathway and only in part modulated by a PI3-kinase pathway.



IGF-I is reported to be expressed during fracture healing and to stimulate it, suggesting a role as an autocrine/paracrine factor potentiating bone regeneration (Trippel 1998). We have investigated the changes in claudin-1 expression in MC3T3-E1 cells during wound healing in vitro as a model of fracture healing in vivo. In MC3T3-E1 cells after scrape wounding, the upregulation of claudin-1 was observed together with increases of IGF-I and type I collagen. This suggests that the upregulation of claudin-1 by IGF-I might occur during not only differentiation but also regeneration of osteoblasts.

In conclusion, during the differentiation of osteoblasts, IGF-I regulates integral membrane tight-junction protein claudin-1 via a MAP-kinase pathway, but not gap junctions. Furthermore, ZO-1, which has been localized at adherens and tight junctions, is induced by IGF-I. In bone, lining cells, which are considered to be resting osteoblasts, cover the inactive surface of mineralized bone and separate it from extracellular space. Osteoblasts in the bone-forming process maintain cell polarity and secrete matrix proteins toward the existing bone surface with exact directionality. It is possible that paracellular permeability between osteoblasts may be modulated by the direct cell-to-cell interactions of tight junctions during differentiation of osteoblasts. Finally, direct cell-to-cell interactions, not only via adherens and gap junctions but also tight junctions, may modulate various osteoblast functions, although the detailed roles of tight junction proteins are as yet unclear in bone cells

## Supplementary Material

Refer to Web version on PubMed Central for supplementary material.

## Acknowledgments

We thank Dr. Kenneth J. McLeod (State University of New York, Stony Brook) and Dr. Lynda F. Bonewald (University of Texas Health Science Center) for graciously providing the MC3T3-E1 and MLO-Y4 cell lines.

This work was supported by Grants-in-Aid from the National Project “Knowledge Cluster Initiative” (2nd stage, “Sapporo Biocluster Bio-s”), the Ministry of Education, Culture, Sports, Science, and Technology, and the Ministry of Health, Labor, and Welfare of Japan, the Akiyama Foundation, and the Japan Science and Technology Agency.

## References

- Arana-Chavez VE, Soares AM, Katchburian E. Junctions between early developing osteoblasts of rat calvaria as revealed by freeze-fracture and ultrathin section electron microscopy. *Arch Histol Cytol* 1995;58:285–292. [PubMed: 8527235]
- Balda MS, Matter K. Epithelial cell adhesion and the regulation of gene expression. *Trends Cell Biol* 2003;13:310. [PubMed: 12791297]
- Bennett MVL, Barrio LC, Bargiello TA, Spray DC, Hertzberg E, Sáez JC. Gap junctions: new tools, new answers, new questions. *Neuron* 1991;6:305–320. [PubMed: 1848077]
- Berthoud VM, Iwanij V, Garcia AM, Sáez JC. Connexins and glucagon receptors during development of rat hepatic acinus. *Am J Physiol* 1992;263:G650–G658. [PubMed: 1332499]
- Canalis E. Insulin like growth factors and local regulation of bone formation. *Bone* 1993;14:273–276. [PubMed: 8363867]
- Chiu D, Ma K, Scott A, Duronio V. Acute activation of Erk1/Erk2 and protein kinase B/akt proceed by independent pathways in multiple cell types. *FEBS J* 2005;272:4372–4384. [PubMed: 16128807]
- Civitelli R, Beyer EC, Warlow PM, Robertson A, Geist ST, Steinberg TH. Connexin 43 mediates direct intercellular communication in human osteoblastic cell networks. *J Clin Invest* 1993;91:1888–1896. [PubMed: 8387535]
- Conover CA. In vitro studies of insulin-like growth factor I and bone. *Growth Horm IGF Res* 2000;10:S107–S110. [PubMed: 10984264]
- D’Atri F, Citi S. Molecular complexity of vertebrate tight junctions. *Mol Membr Biol* 2002;19:103–112. [PubMed: 12126228]

- Farquharson C, Milne J, Loveridge N. Mitogenic action of insulin-like growth factor-I on human osteosarcoma MG-63 cells and rat osteoblasts maintained in situ: the role of glucose-6-phosphate dehydrogenase. *Bone Miner* 1993;22:105–115. [PubMed: 8251763]
- Franz-Odenaal TA, Hall BK, Witten PE. Buried alive: how osteoblasts become osteocytes. *Dev Dyn* 2006;235:176–190. [PubMed: 16258960]
- Furuse M, Hirase T, Itoh M, Nagafuchi A, Yonemura S, Tsukita S, Tsukita S. Occludin: a novel integral membrane protein localizing at tight junctions. *J Cell Biol* 1993;123:1777–1788. [PubMed: 8276896]
- Furuse M, Furuse K, Sasaki H, Tsukita S. Conversion of zonulae occludentes from tight to leaky strand type by introducing claudin-2 into Madin-Darby canine kidney I cells. *J Cell Biol* 2001;153:263–272. [PubMed: 11309408]
- Giepmans BNG. Gap junctions and connexin-interacting proteins. *Cardiovasc Res* 2004;62:233–245. [PubMed: 15094344]
- Go M, Kojima T, Takano K, Murata M, Koizumi J, Kurose M, Kamekura R, Osanai M, Chiba H, Spray DC, Himi T, Sawada N. Connexin 26 expression prevents down-regulation of barrier and fence functions of tight junctions by  $\text{Na}^+/\text{K}^+$ -ATPase inhibitor ouabain in human airway epithelial cell line Calu-3. *Exp Cell Res* 2006;312:3847–3856. [PubMed: 16982053]
- Grey A, Chen Q, Callon K, Xu X, Cornish J. Parallel phosphatidylinositol-3 kinase and p42/44 mitogen-activated protein kinase signaling pathways subserve the mitogenic and antiapoptotic actions of insulin-like growth factor I in osteoblastic cells. *Endocrinology* 2003;144:4886–4893. [PubMed: 12960100]
- Gu G, Nars M, Hentunen TA, Metsikkö K, Väänänen HK. Isolated primary osteocytes express functional gap junctions in vitro. *Cell Tissue Res* 2006;323:263–271. [PubMed: 16175387]
- Hanai Y, Tokuda H, Ishisaki A, Matsushima-Nishiwaki R, Nakamura N, Yoshida M, Takai S, Kozawa O. Involvement of p44/p42 MAP kinase in insulin-like growth factor-I-induced alkaline phosphatase activity in osteoblast-like-MC3T3-E1 cells. *Mol Cell Endocrinol* 2006;251:42–48. [PubMed: 16616413]
- Ikenouchi J, Furuse M, Furuse K, Sasaki H, Tsukita S, Tsukita S. Tricellulin constitutes a novel barrier at tricellular contacts of epithelial cells. *J Cell Biol* 2005;171:939–945. [PubMed: 16365161]
- Inai T, Kobayashi J, Shibata Y. Claudin-1 contributes to the epithelial barrier function in MDCK cells. *Eur J Cell Biol* 1999;78:849–855. [PubMed: 10669103]
- Kojima T, Sawada N, Duffy HS, Spray DC. Gap and tight junctions in liver: composition, regulation and function. In: Arias IM, Boyer JL, Chisari FV, Fausto N, Schachter D, Shafritz DA, editors. *The liver: biology and pathobiology*. Vol. 4. Lippincott Williams & Wilkins; Philadelphia: 2001. p. 29–46.
- Kojima T, Spray DC, Kokai Y, Chiba H, Mochizuki Y, Sawada N. Cx32 formation and/or Cx32-mediated intercellular communication induces expression and function of tight junctions in hepatocytic cell line. *Exp Cell Res* 2002;276:40–51. [PubMed: 11978007]
- Kojima T, Yamamoto T, Murata M, Chiba H, Kokai Y, Sawada N. Regulation of the blood-biliary barrier: interaction between gap and tight junctions in hepatocytes. *Med Electron Microsc* 2003;36:157–164. [PubMed: 14505059]
- Kojima T, Murata M, Go M, Spray DC, Sawada N. Connexins induce and maintain tight junctions in epithelial cells. *J Membr Biol* 2007;217:13–19. [PubMed: 17568974]
- Kumar NM, Gilula NB. The gap junction communication channel. *Cell* 1996;84:381–388. [PubMed: 8608591]
- Laing JG, Manley-Markowski RN, Koval M, Civitelli R, Steinberg TH. Connexin45 interacts with zonula occludens-1 and connexin43 in osteoblastic cells. *J Biol Chem* 2001;276:23051–23055. [PubMed: 11313345]
- Laron Z, Klinger B, Silbergeld A. Patients with Laron syndrome have osteopenia/osteoporosis. *J Bone Miner Res* 1999;14:156–157. [PubMed: 9893081]
- Laviola L, Natalicchio A, Giordano F. The IGF-I signaling pathway. *Curr Pharm Des* 2007;13:663–669. [PubMed: 17346182]
- LeRoith D. Insulin-like growth factor I receptor signaling—overlapping or redundant pathways? *Endocrinology* 2000;141:1287–1288. [PubMed: 10746630]

- Li Z, Zhou Z, Saunders MM, Donahue HJ. Modulation of connexin43 alters expression of osteoblastic differentiation markers. *Am J Physiol Cell Physiol* 2006;290:C1248–C1255. [PubMed: 16319124]
- Loewenstein WR. Junctional intercellular communication and the control of growth. *Biochim Biophys Acta* 1979;560:1–65. [PubMed: 216404]
- McCarthy TL, Centrella M, Canalis E. Regulatory effects of insulin-like growth factors I and II on bone collagen synthesis in rat calvarial cultures. *Endocrinology* 1989;124:301–309. [PubMed: 2909370]
- Moelling K, Schad K, Bosse M, Zimmermann S, Schweneker M. Regulation of Raf-Akt cross-talk. *J Biol Chem* 2002;277:31099–31106. [PubMed: 12048182]
- Morita H, Katsuno T, Hoshimoto A, Hirano N, Saito Y, Suzuki Y. Connexin 26-mediated gap junctional intercellular communication suppresses paracellular permeability of human intestinal epithelial cell monolayers. *Exp Cell Res* 2004;298:1–8. [PubMed: 15242756]
- Noda T, Tokuda H, Yoshida M, Yasuda E, Hanai Y, Takai S, Kozawa O. Possible involvement of phosphatidylinositol 2-kinase/Akt pathway in insulin-like growth factor-I-induced alkaline phosphatase activity in osteoblasts. *Horm Metab Res* 2005;37:270–274. [PubMed: 15971148]
- Olney RC. Regulation of bone mass by growth hormone. *Med Pediatr Oncol* 2003;41:228–234. [PubMed: 12868124]
- Pei Y, Meng XW, Zhou XY, Xing XP, Xia WB. Expression of core binding factor  $\alpha 1$  up-regulated by IGF-I, GM-CSF, and EGF through MAPK pathway in MC3T3-E1 and C2C12 cells. *Acta Pharmacol Sin* 2003;24:975–984. [PubMed: 14531938]
- Prêle CM, Horton MA, Caterina P, Stenbeck G. Identification of the molecular mechanisms contributing to polarized trafficking in osteoblasts. *Exp Cell Res* 2003;282:24–34. [PubMed: 12490191]
- Reusch HP, Zimmermann S, Schaefer M, Paul M, Moelling K. Regulation of Raf by Akt controls growth and differentiation in vascular smooth muscle cells. *J Biol Chem* 2001;276:33630–33637. [PubMed: 11443134]
- Rommel C, Clarke BA, Zimmermann S, Nuñez L, Rossman R, Reid K, Moelling K, Yancopoulos GD, Glass DJ. Differentiation stage-specific inhibition of the Raf-MEK-ERK pathway by Akt. *Science* 1999;286:1738–1741. [PubMed: 10576741]
- Sáez JC, Spray DC, Nairn AC, Hertzberg E, Greengard P, Bennett MV. cAMP increases junctional conductance and stimulates phosphorylation of the 27-kDa principal gap junction polypeptide. *Proc Natl Acad Sci USA* 1986;83:2473–2477. [PubMed: 3010311]
- Sáez JC, Conner JA, Spray DC, Bennett MV. Hepatocyte gap junctions are permeable to the second messenger, inositol 1,4,5-trisphosphate, and to calcium ions. *Proc Natl Acad Sci USA* 1989;86:2708–2712. [PubMed: 2784857]
- Saitou M, Furuse M, Sasaki H, Schulzke JD, Fromm M, Takano H, Noda T, Tsukita S. Complex phenotype of mice lacking occludin, a component of tight junction strands. *Mol Biol Cell* 2000;11:4131–4142. [PubMed: 11102513]
- Sawada N, Murata M, Kikuchi K, Osanai M, Tobioka H, Kojima T, Chiba H. Tight junctions and human diseases. *Med Electron Microsc* 2003;36:147–156. [PubMed: 14505058]
- Schiller PC, Mehta PP, Ross BA, Howard GA. Hormonal regulation of intercellular communication: parathyroid hormone increases connexin 43 gene expression and gap-junctional communication in osteoblastic cells. *Mol Endocrinol* 1992;6:1433–1440. [PubMed: 1331776]
- Schirmmacher K, Schmitz I, Winterhager E, Traub O, Brummer F, Jones D, Bingmann D. Characterization of gap junctions between osteoblast-like cells in culture. *Calcif Tissue Int* 1992;51:285–290. [PubMed: 1330238]
- Schneeberger EE, Lynch RD. The tight junction: a multifunctional complex. *Am J Physiol Cell Physiol* 2004;286:C1213–C1228. [PubMed: 15151915]
- Soares AM, Arana-Chavez VE, Reid AR, Katchburian E. Lanthanum tracer and freeze-fracture studies suggest that compartmentalization of early bone matrix may be related to initial mineralisation. *J Anat* 1992;181:345–356. [PubMed: 1295872]
- Stains JP, Civitelli R. Cell-cell interactions in regulating osteogenesis and osteoblast function. *Birth Defects Res C Embryo Today* 2005;1:72–80. [PubMed: 15838921]
- Steinberg TH, Civitelli R, Geist ST, Robertson AJ, Hick E, Veenstra RD, Wang HZ, Warlow PM, Westphale EM, Laing JG, Beyer EC. Connexin 43 and connexin 45 from gap junctions with different molecular permeabilities in osteoblastic cells. *EMBO J* 1994;13:744–750. [PubMed: 8112289]

- Thi MM, Kojima T, Cowin SC, Weinbaum S, Spray DC. Fluid shear stress remodels expression and function of junctional proteins in cultured bone cells. *Am J Physiol Cell Physiol* 2003;284:C389–C403. [PubMed: 12388096]
- Trippel SB. Potential role of insulinlike growth factors in fracture healing. *Clin Orthop Relat Res* 1998;355:S301–S313. [PubMed: 9917650]
- Trosko JE, Ruch RJ. Cell-cell communication in carcinogenesis. *Front Biosci* 1998;3:D208–D236. [PubMed: 9458335]
- Tsukita S, Furuse M. Claudin-based barrier in simple and stratified cellular sheets. *Curr Opin Cell Biol* 2002;14:531–536. [PubMed: 12231346]
- Tsukita S, Furuse M, Itoh M. Multifunctional strands in tight junctions. *Nat Rev Mol Cell Biol* 2001;2:285–293. [PubMed: 11283726]
- Wongdee K, Pandaranandaka J, Teerapornpantakit J, Tudpor K, Thongbunchoo J, Thongon N, Jantarajit W, Krishnamra N, Charoenphandhu N. Osteoblasts express claudins and tight junction-associated proteins. *Histochem Cell Biol* 2008;130:79–90. [PubMed: 18365232]
- Yamasaki H, Naus CC. Role of connexin genes in growth control. *Carcinogenesis* 1996;17:1199–1213. [PubMed: 8681433]
- Zhang W, Lee JC, Kumar S, Gowen M. ERK pathway mediates the activation of Cdk2 in IGF-1-induced proliferation of human osteosarcoma MG-63 cells. *J Bone Miner Res* 1999;14:528–535. [PubMed: 10234573]
- Zimmermann S, Moelling K. Phosphorylation and regulation of Raf by Akt (protein kinase B). *Science* 1999;286:1741–1744. [PubMed: 10576742]

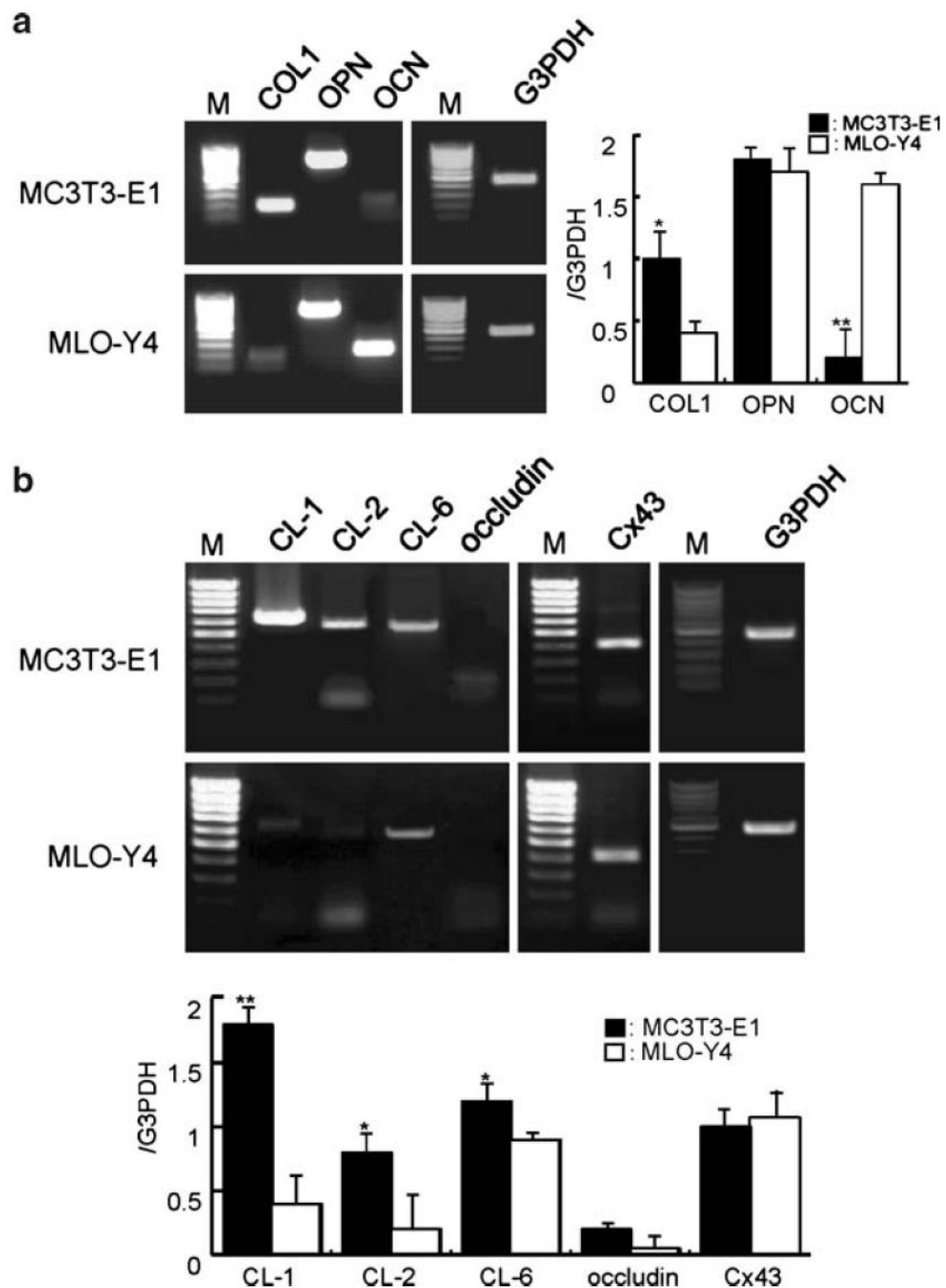


**Fig. 1.** Expression of osteoblast differentiation markers (**a**), tight-junction molecules (**b**), and connexin 43 (*Cx43* in **b**) in MC3T3-E1 cells and MLO-Y4 cells. **a** Reverse transcription with polymerase chain reaction (RT-PCR) for mRNAs of type I collagen (*COL1*), osteopontin (*OPN*), and osteocalcin (*OCN*) in MC3T3-E1 cells and MLO-Y4 cells (*M* 100-bp ladder DNA marker). The corresponding expression levels of *COL1*, *OPN*, and *OCN* mRNAs relative to glucose-3-phosphate dehydrogenase (*G3PDH*) are shown in a bar graph (right). \*\* $P < 0.01$ , \* $P < 0.05$  versus MLO-Y4 cells. **b** RT-PCR for mRNAs of various claudins (*CL-1*, *CL-2*, *CL-6*), occludin, and *Cx43* in MC3T3-E1 cells and MLO-Y4 cells. The corresponding

expression levels of claudin-1, -2, and-6, occludin, and Cx43 mRNAs relative to G3PDH are shown in a *bar graph (bottom)*. \*\* $P < 0.01$ , \* $P < 0.05$  versus MLO-Y4 cells

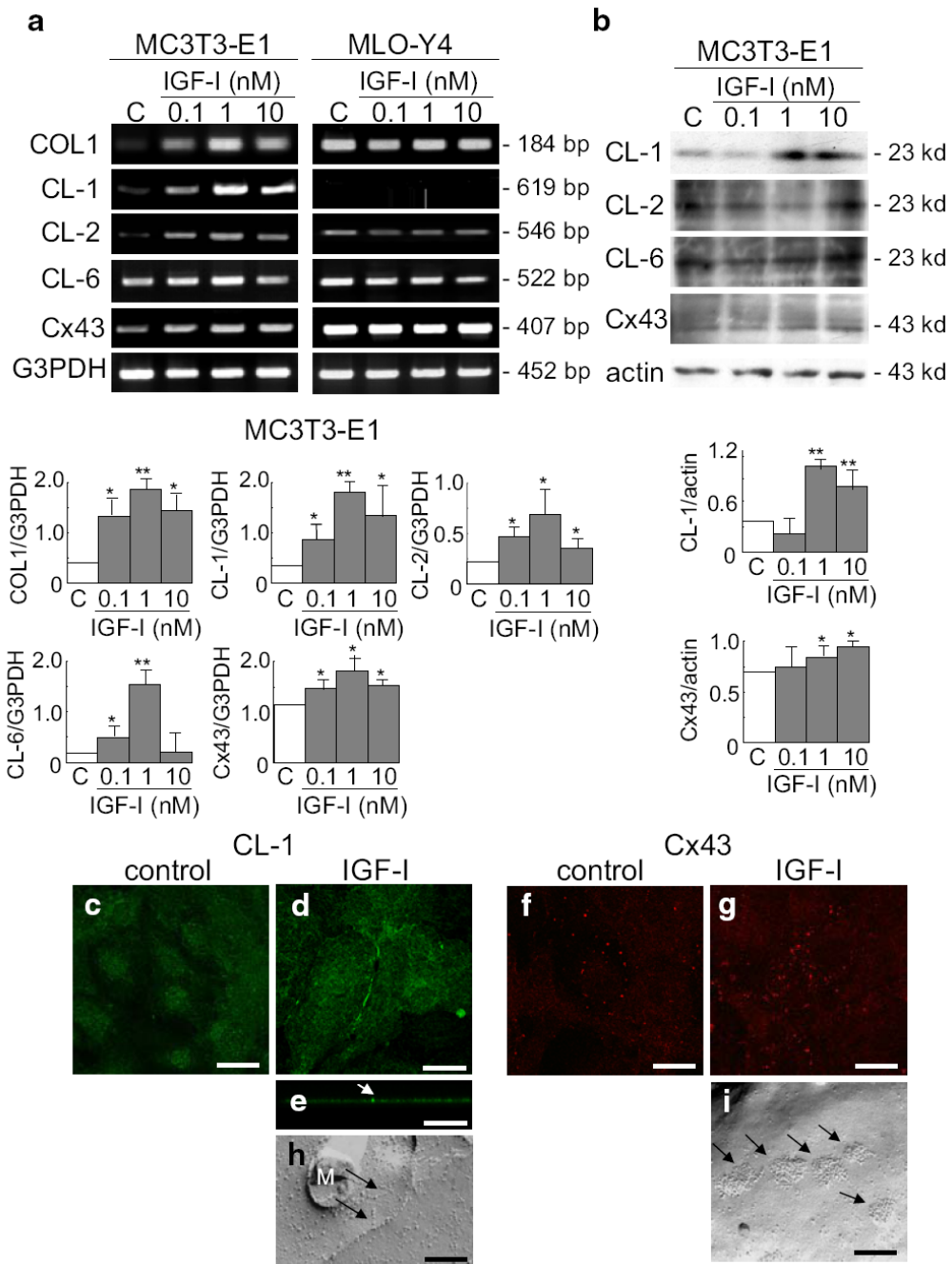


**Fig. 2.** Changes in type I collagen (*COL1*), various claudins, and connexin 43 (*Cx43*) in MC3T3-E1 cells and MLO-Y4 cells after treatment with IGF-I. **a** RT-PCR for mRNAs of COL1, claudin-1 (*CL-1*), claudin-2 (*CL-2*), claudin-6 (*CL-6*), and Cx43 in MC3T3-E1 cells and MLO-Y4 cells after treatment with 0.1–10 nM IGF-I for 24 h. In MC3T3-E1, but not in MLO-Y4, upregulation in mRNAs of claudin-1, -2, -6 and Cx43 was observed after treatment with 0.1 nM IGF-I. The corresponding expression levels of COL1, claudin-1, -2, -6, and Cx43 mRNAs in MC3T3-E1 cells are shown in a *bar graph*. \*\* $P < 0.01$ , \* $P < 0.05$  versus control. **b** Western blotting for claudin-1, -2, -6, and Cx43 proteins in MC3T3-E1 cells after treatment with 0.1–10 nM IGF-I. In MC3T3-E1 cells, upregulation of claudin-1 and Cx43 proteins was observed from 1 nM

IGF-I. The corresponding expression levels of claudin-1 and Cx43 proteins are shown in a *bar graph*. \*\* $P < 0.01$ , \* $P < 0.05$  versus control. **c–g** Immunocytochemistry for claudin-1 (**c–e**) and Cx43 (**f, g**) in MC3T3-E1 cells after treatment with 1 nM IGF-I. Claudin-1-immunoreactive lines were detected at cell borders, and Cx43-positive spots were increased compared with control. (**c, d, f, g** XY-sections, **e** Z-section, *arrow* in **e** claudin-1-immunoreactive dot. *Bars* 20  $\mu\text{m}$ . **h, i** Freeze-fracture replicas of MC3T3-E1 cells after treatment with 1 nM IGF-I. Several short tight-junction-like strands and many typical gap-junction plaques were observed at the cell membrane (*M* microvilli, *arrows* in **h** tight-junction-like strands, *arrows* in **i** gap-junction plaques). *Bars* 20 nm



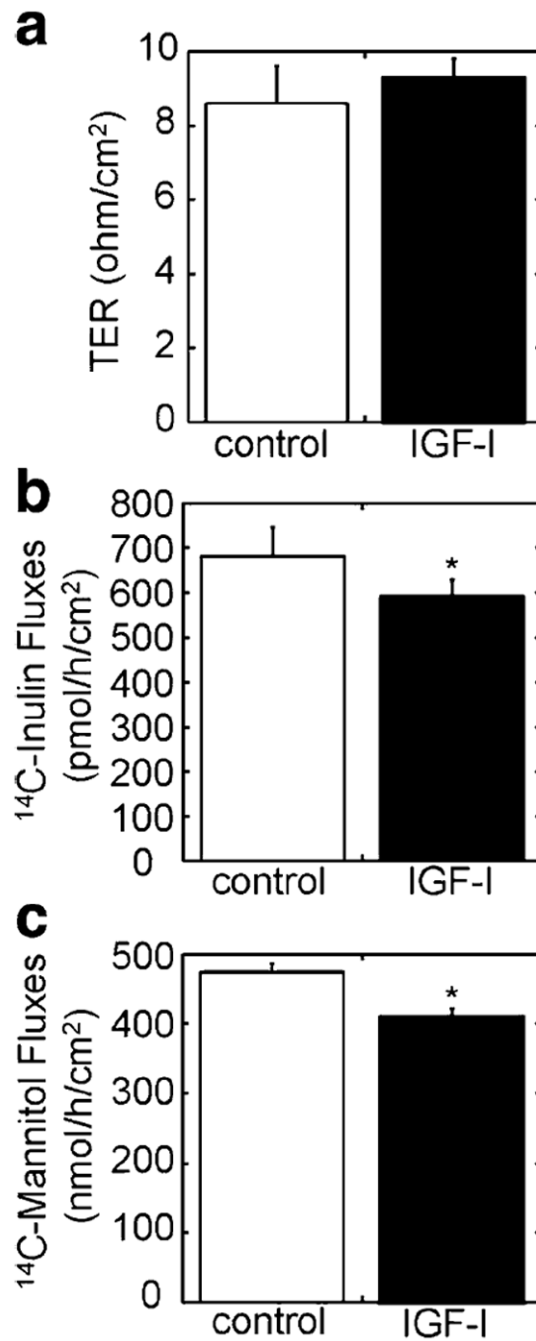


**Fig. 3.** Changes in paracellular permeability of tight junctions in MC3T3-E1 after treatment with IGF-I. **a** Barrier function measured as TER in MC3T3-E1 cells after treatment with 1 nM IGF-I;  $n=9$ . **b** Paracellular permeability assay measured as paracellular fluxes by using <sup>14</sup>C-inulin (MW: 5 kDa) and <sup>14</sup>C-mannitol (MW: 182 Da) in MC3T3-E1 cells after treatment with 1 nM IGF-I;  $n=9$ , \* $P<0.01$  versus control

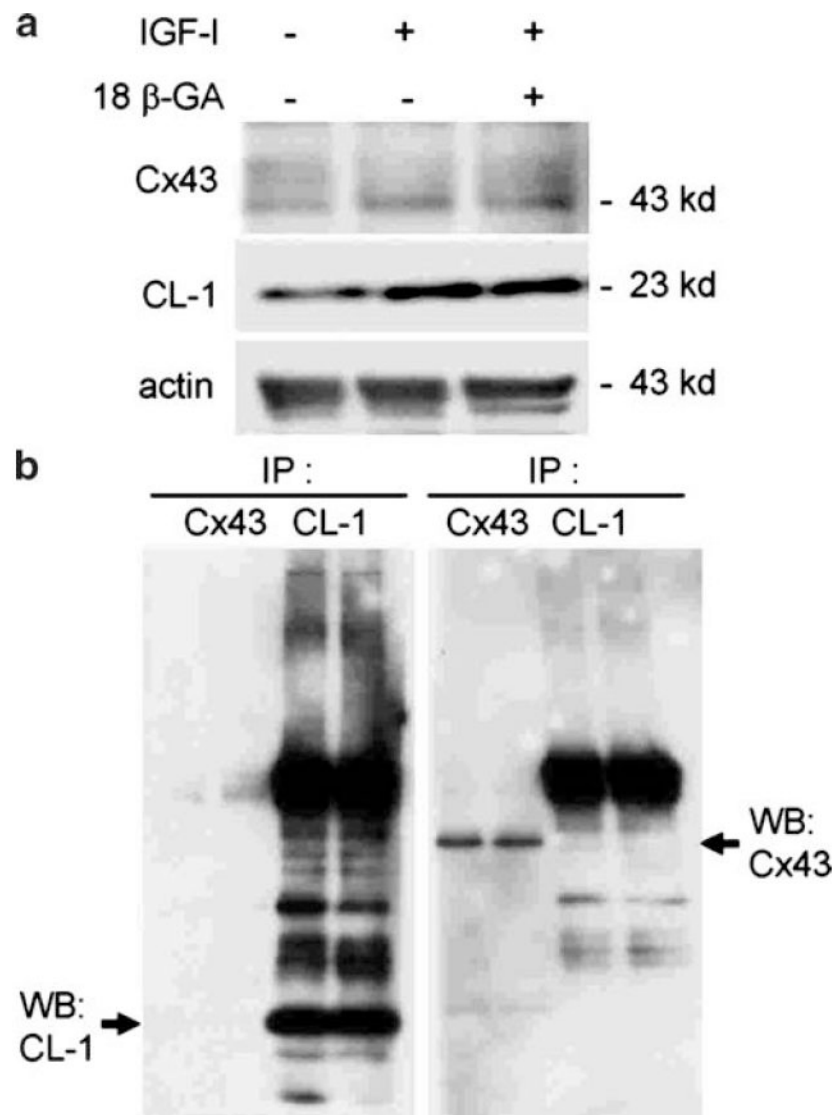


**Fig. 4.** Interaction between connexin 43 (*Cx43*) and claudin-1 (*CL-1*) in MC3T3-E1 after treatment with IGF-I (*kd* kDa). **a** Western blotting for Cx43 and claudin-1 proteins in MC3T3-E1 treated with 10  $\mu$ M 18 $\beta$ -glycyrrhetic acid (18 $\beta$ -GA) for 24 h before treatment with 1 nM IGF-I for 24 h. 18 $\beta$ -GA did not prevent the increase of claudin-1 in MC3T3-E1 cells treated with IGF-I. **b** Immunoprecipitation (IP) and Western blotting (WB) for Cx43 and claudin-1 proteins in MC3T3-E1 after treatment with 1 nM IGF-I. No Cx43 and claudin-1 were detected in immunoprecipitates by using the relevant antibodies, Cx43 and CL-1 were not detected

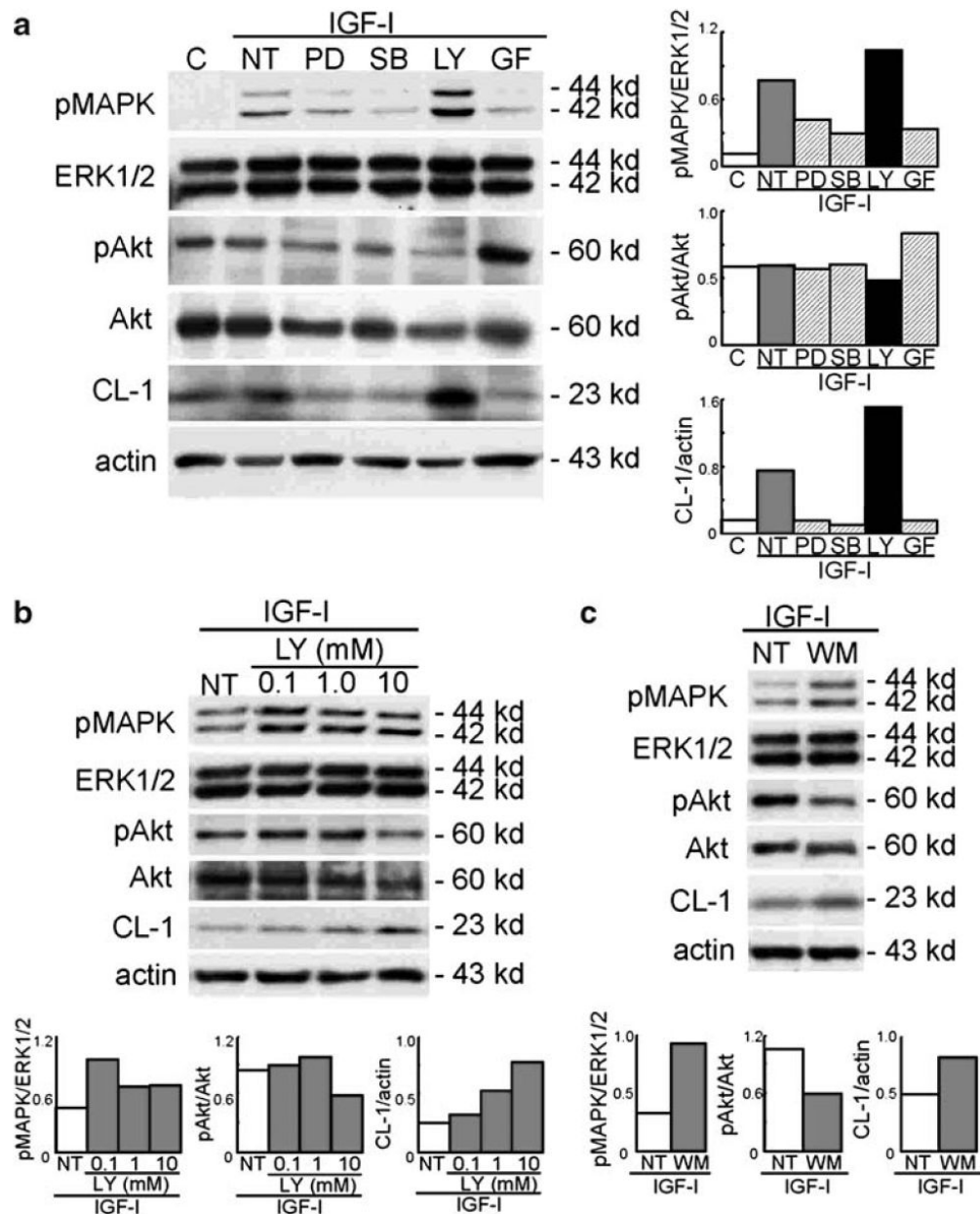


**Fig. 5.** Effects of signaling transduction inhibitors for upregulation of claudin-1 (*CL-1*) protein in MC3T3-E1 cells after treatment with IGF-I (*kd* kDa). **a** Western blotting for pMAPK, ERK1/2, pAkt, Akt, and claudin-1 proteins in MC3T3-E1 cells treated with MAP-kinase inhibitor PD98059 (*PD*), p38 MAP-kinase inhibitor SB203580 (*SB*), PI3-kinase inhibitor LY294002 (*LY*), or protein kinase C inhibitor GF109203 (*GF*) at 10  $\mu$ M for 30 min before treatment with 1 nM IGF-I for 24 h. The corresponding expression levels of pMAPK/ERK1/2, pAkt/Akt, and claudin-1/actin are shown in *bar graphs* (C control, NT non-treatment of inhibitors). **b** Western blotting for pMAPK, ERK1/2, pAkt, Akt, and claudin-1 proteins in MC3T3-E1 cells treated with 0.1–10  $\mu$ M LY294002 before treatment with 1 nM IGF-I. The corresponding expression levels of pMAPK/ERK1/2, pAkt/Akt, and claudin-1/actin are shown in *bar graphs*. **c** Western blotting for pMAPK, ERK1/2, pAkt, Akt, and claudin-1 proteins in MC3T3-E1 cells treated

with 10 nM PI3-kinase inhibitor wortmannin (*WM*) before treatment with 1 nM IGF-I. The corresponding expression levels of pMAPK/ERK1/2, pAkt/Akt, and claudin-1/actin are shown as *bar graphs*

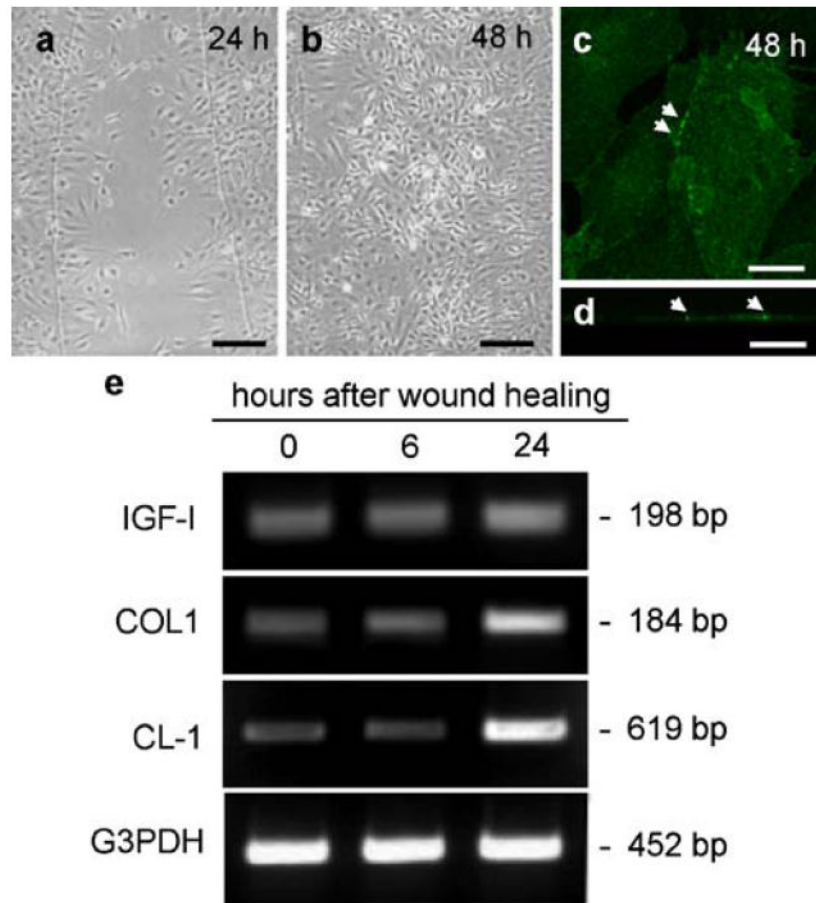


**Fig. 6.** Changes in claudin-1 (*CL-1*) in MC3T3-E1 cells during wound healing. **a, b** Phase-contrast images of MC3T3-E1 cells at 24 h and 48 h after scrape wounding. Bars 50  $\mu$ m. **c, d** Immunocytochemistry for claudin-1 in MC3T3-E1 cells at 48 h after scrape wounding (**c** XY-section, **d** Z-section, arrows claudin-1-immunoreactive dots). Bars 15  $\mu$ m (**a, b**), 10  $\mu$ m (**c, d**). **e** RT-PCR for IGF-I, type I collagen (*COL1*), claudin-1 (*CL-1*) in MC3T3-E1 cells at 6 h and 24 h after scrape wounding

Table 1

## Primers for PCR

Gene	Forward primer	Reverse primer	Product size (bp)
Type I collagen	AATGGTGAGACGTGGAAAACCCGAG	CGACTCCTACATCTTCTGAGTTTGG	184
Osteopontin	GACCATGAGATTGACAGATTTG	TGATGTTCCAGGGTGCACAGAGTTTG	765
Osteocalcin	GACAAAGCCTTTCATGTCCAAAGC	AAAGCCGCTGCCAGAGTTTG	240
Occludin	TCAGGGAATATCCACCTATCACTTCAG	CATCAGCAGCAGCCATGTACTCTTCAC	136
Claudin-1	TCTAGAAAGAGCCATGGCCAACG	TCTAGATCACACATAGTCTTTCCCCAC	619
Claudin-2	GCTCTAGAGGTCTGCCATGGCCTC	GCTCTAGATCACACATACCCAGTC	546
Claudin-3	TCTAGAGCCGCCACCATGTCCATGGGCTG	TCTAGATCAGAGGTAGTCCCTTGCGG	511
Claudin-4	GCTCTAGAGCCGCCACCATGGCGTCTATG	GCTCTAGATCACACATAGTTGTGCTGGC	430
Claudin-5	GAATTCGCCGCCACCATGGGGTCTGCAGCGTTG	GAATTCCTCAGACATAGTCTTCTTGTCTGTAATCG	612
Claudin-6	TCTAGAGCCGCCACCATGGCCTTACTGG	TCTAGATCACACATAATCTTGGTGGG	522
Claudin-7	TCTAGAGCCGCCACCATGGCCAACTCGGG	TCTAGATCACACGTATTCCTTGGGAGG	496
Claudin-8	TCTAGAGCCGCCACCATGGCAAACCTACGCC	TCTAGATCACACATACTGACTTTTGG	610
Connexin 43	TACCACGCCACCACTGGC	AATCTCCAGGTCAATCAGG	407
Glucose-3-phosphate dehydrogenase	ACCACAGTCCATGGCCATCA	TCCACCACCCCTGTTGCTGTA	452